Mem. S.A.It. Vol. 93, 34

Memorie della

The Extragalactic Population of Accreting Neutron Stars and the Ultraluminous X-ray Sources Paradigm: from ULTraS to PULSULTraS

G. L. Israel[1], A. De Luca[2], M. Bachetti[3], A. Belfiore[2], P. Esposito[4], M. Imbrogno[5,1], A. Miraval Zanon[1], F. Pisanu[6], G. A. Rodríguez Castillo[7], R. Salvaterra[2], A. Tiengo[2,4,8], and A. Wolter[9], and on behalf of the ULTraS and PULSULTraS teams

[1] Istituto Nazionale di Astrofisica (INAF) – Osservatorio Astronomico di Roma, Via Frascati 33, I-00078 Monte Porzio Catone, Italy, e-mail: gianluca.israel@inaf.it
[2] INAF – Istituto di Astrofisica Spaziale e Fisica Cosmica Milano, Via A. Corti 12, I-20133 Milano, Italy
[3] INAF-Osservatorio Astronomico di Cagliari, Via della Scienza 5, I-09047 Selargius (CA), Italy
[4] Scuola Universitaria Superiore IUSS Pavia, Piazza della Vittoria 15, 27100 Pavia, Italy
[5] Dipartimento di Fisica, Università degli Studi di Roma "Tor Vergata," via della Ricerca Scientifica, 1, I-00133 Roma, Italy
[6] LIPN, CNRS, Université Sorbonne Paris Nord, 93430 Villeaneuse, France.
[7] INAF – Istituto di Astrofisica Spaziale e Fisica Cosmica di Palermo, Via U. La Malfa 153, I-90146 Palermo, Italy
[8] Istituto Nazionale di Fisica Nucleare, Sezione di Pavia, via A. Bassi 6, I-27100 Pavia, Italy
[9] INAF-Osservatorio Astronomico di Brera, Via Brera 28, I-20121 Milano, Italy

Received: 31 December 2021; Accepted: 19 May 2022

Abstract. The unambiguous identification of the nature of a neutron star in X-rays is achieved through the detection of coherent signals reflecting the spin period of the compact object. The search for coherent signals in the whole XMM-Newton source catalog was one of the main aims of the EU/FP7-funded project *EXTraS* (active in 2014-2016). The ULTraS and PULSULTraS projects start from the findings achieved by *EXTraS* and concerning the X-ray pulsars identified in the Andromeda Galaxy and among the class of Ultraluminous X-ray Sources (ULXs). In particular, we focused on the development of data analysis tools able to account for the extreme timing properties of pulsars moving in binary orbits and accreting at super-Eddington rates, i.e with very high first period derivative values, that made their discovery elusive. Part of these tools are becoming available to the whole community through their inclusion in the `Stingray` software package. Then, we searched for new extragalactic pulsars by applying the new developed timing tools to both archival data and a dedicated XMM-Newton Large Program: we discovered a new pulsating ULX in M51, the first pulsar in a low mass binary in M31, and twelve further pulsators of different nature (neutron stars and white dwarfs). At the same time we studied in great details the timing properties of the already known pulsating ULXs (M82 X-2, NGC7793 P13 and NGC5907 ULX-1).

Key words. Pulsars: general – Stars: neutron – Accretion, accretion disks – Catalogs – X-rays: binaries – X-rays: galaxies – Methods: data analysis

1. Introduction

The work was performed within the frame of the two projects "ULTraS" (PI A. De Luca) and "PULSULTraS" (PI G.L. Israel) funded within the first and second call, respectively, of the ASI-INAF agreement n.2017-14-H.0. The paper of De Luca et al. focus on aperiodic, short term variability studies, mainly based on a systematic data mining approach, with results encompassing a broad diversity of astrophysical sources. In this paper we focus on the search for coherent signals, with particular emphasis on results that changed our view of Ultraluminous X-ray Sources (ULXs) and, more in general, of the extragalactic population of accreting neutron stars.

X-ray pulsars are a perfect laboratory where to study the properties of accreting matter, its interaction with the magnetic field of neutron stars (NSs), and the transfer of the angular momentum. The largest majority of known accreting X-ray pulsars are found in high mass binary systems (HMXBs) with young OB spectral-type companion stars, either (super)giant or Be type stars. Depending on the companion spectral-type different transfer channels are foreseen: fast and radial stellar wind in (super)giant systems and a slow and dense circumstellar disk along the orbital plane in the Be binaries. The accretion channel is also responsible for the variability properties of X-ray pulsars in HMXBs. In fact, accreting pulsars with supergiant companions are mainly observed as relatively bright (up to 10^{38} erg s^{-1}) persistent X-ray sources, while Be systems are often transients or highly variable sources (with L_X ranging in the 10^{34}-10^{38} erg s^{-1}).

Despite the large observational effort carried out since the '80s in searching for X-ray pulsars outside the Milky Way and the Magellanic Clouds (mainly due to a combination of limited sensitivity and angular/time resolution of past X-ray missions), only in 2007 the first unambiguous extra-galactic accreting and pulsating neutron star, with a period of ∼18 s, was discovered (Trudolyubov, Priedhorsky, & Córdova , 2007) in the nearby spiral galaxy NGC 2403 . This first X-ray pulsar, discovered thanks to the XMM-Newton/Chandra missions, was later followed by a ∼ 756 s transient pulsar in NGC 1313 and a 285 s transient pulsar in M 33 (Trudolyubov , 2008, 2013). It is worth noticing that these first discovered pulsars were already suggesting objects with extreme physical properties, a first period derivative ($\dot{P}$) of -10^{-7} for the NS in NGC 2403 and a luminosity in excess of 10^{39} erg s^{-1} for the NSs in NGC 2403 and NGC 1313.

In 2014 a bright, 10^{39} <L_X(erg s^{-1})<10^{40}, ∼1.4 s-period pulsar hosted in a 2.5 days orbital period system was discovered owing to *NuSTAR* observations (M 82 X-2 at a distance of 3.6 Mpc; Bachetti et al. 2014). Due to its characteristics it became the prototype of the pulsating Ultraluminous X-ray Sources (PULXs) class.

Ultraluminous X-ray sources are off-nuclear objects detected in nearby galaxies with X-ray luminosities in excess of 10^{39} erg s^{-1}, which is the Eddington luminosity ($L_{\rm Edd}$) for a black hole (BH) of 10 $M_\odot$. $L_{\rm Edd}$ sets the upper limit to the accretion luminosity ($L_{\rm acc}$) that a compact object can steadily produce, since for $L_{\rm acc} > L_{\rm Edd}$, the accretion flow is halted by the radiation pressure. For spherical accretion of fully ionized hydrogen, the limit can be written as $L_{\rm Edd} = 4\pi cGMm_{\rm p}/\sigma_{\rm T} \simeq 1.3 \times 10^{38}(M/M_\odot)$ erg s^{-1}, where $\sigma_{\rm T}$ is the Thomson scattering cross section, $m_{\rm p}$ is the proton mass, and $M/M_\odot$ is the compact object mass in solar masses; for a 1.4 $M_\odot$ neutron star (NS), the maximum accreting luminosity is ∼ 2×10^{38} erg s^{-1}. Since their discovery in the '70s with the Einstein mission, the high luminosity of ULXs has thus been interpreted as accretion at or above the Eddington luminosity onto BHs of stellar origin (<80–100 $M_\odot$), or onto intermediate-mass (10^3–10^5 $M_\odot$) BHs.

2. EXTraS and its heritage

During 2014–16 the project called Exploring the X-ray transient and variable sky (hereafter *EXtraS*) was funded by the European Union within the Seventh Framework Programme (FP7-Space) with the main aim of systematically extracting all temporal domain information in the XMM-Newton archive. *EXtraS* was

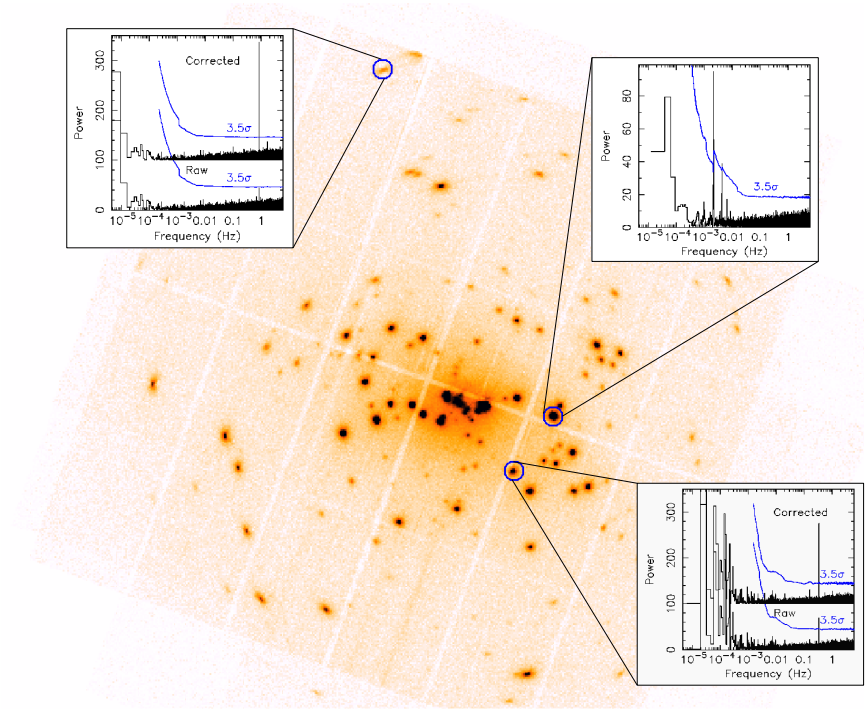

Fig. 1. XMM pn plus MOSs cleaned image of ObsId 0112570101 (64ks effective exposure time) for the galaxy M31. The insets show the pn power spectra (solid black lines) together with the local 3.5σ detection threshold (solid blue lines) obtained from the unbinned event lists of the two pulsating sources discovered during the EXTraS project, 3XMM J004301.4+413017 and 3XMM J004222.9+411535 (upper insets), and the new pulsar discovered after the end of the project, 3XMM J004232.1+411314 (bottom inset). In the cases of J004301 and J004232, the discovered X-ray pulsars revolve around a companion star. In the corresponding insets we show the power spectra with (corrected) and without (raw) the best inferred orbital corrections (shifted by 100 in power on the y-axis for clarity). Adapted from De Luca et al. (2021).

aimed at searching and characterising the variability, both periodic and aperiodic, of hundreds of thousands of sources spanning more than eight orders of magnitude in timescale and six orders of magnitude in flux, and a search for fast transients that were missed by standard image analysis (see De Luca et al. 2021 and the dedicated web page[1] for the details of the project and its public products). Focusing on the periodic variability search, within the *EXtraS* project more than 40 new X-ray pulsators were discovered with coherent signals in the 400ms–3hr range. Among these objects are two new PULXs (namely NGC 5907 ULX-1 Israel et al. 2017a and NGC 7793 P13 Israel et al. 2017b, see also Fürst et al. 2016; the former one is also the farthest and brightest pulsar ever discovered). The first accreting X-ray pulsar, with 1.2 s-period, in the nearby Andromeda galaxy (Esposito et al. 2016; see also Zolotukhin et al. 2017) was also discovered (see Figure 1) hosted in a 1.2 day orbital period binary system.

The discovery of two further PULXs demonstrates that accreting NSs can achieve extreme luminosities, above 500 times the $L_{\rm Edd}$ (in the most extreme case), which is simply not

[1] http://www.extras-fp7.eu/

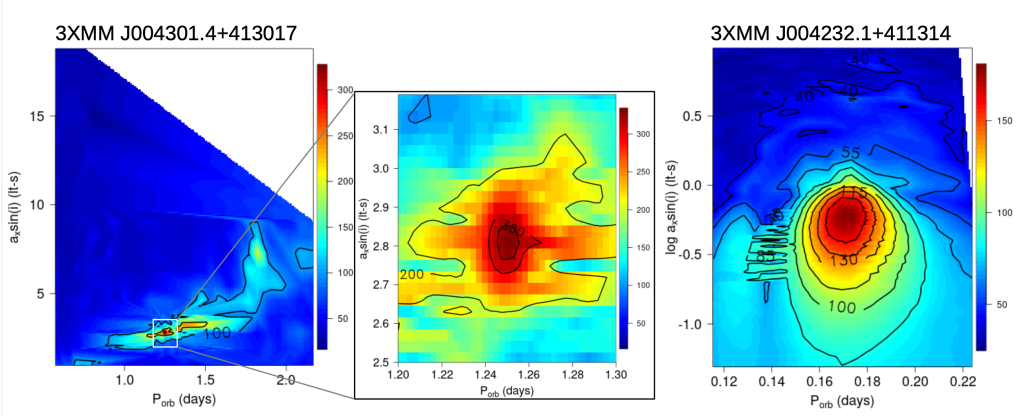

Fig. 2. Results obtained by applying the new timing tools taking into account both the orbital and $\dot{P}$ corrections to the archival XMM-Newton datasets of M31. In particular, the plane P_{orb} versus $a_x sin\, i$ is shown for the already known 1.2 s pulsars 3XMM J004301.4+413017 hosted in a binary system with P_{orb} ∼1.27 day and $a_x sin\, i$ ∼2.9 lt-s (left and central panels) and for the newly discovered 3 s pulsars 3XMM J004232.1+411314 with P_{orb} ∼0.17 day and Log[$a_x sin\, i$] ∼-0.22 lt-s. Colors mark the Leahy power estimates in the corresponding PSD (see intensity scales on the right).

conceivable in the current accretion models. Different scenarios have been proposed and the presence of a strong multipolar magnetic field (∼10^{14} G) close to the surface of the NSs appears a reasonable way out of the problem (Israel et al. , 2017a; Chashkina, Abolmasov, & Poutanen , 2017), though "standard" magnetic fields of ∼10^{12} G and high beaming factor of the emitted radiation are not excluded.

Another important consequence of the discovery of these PULXs is that the nature of many ULXs which have been classified in good faith as accreting black holes due to their high luminosity is now in doubt. An unknown but possibly large fraction of ULXs might host an accreting NS rather than a BH. The latter issue has strong impact on many topics beyond compact object studies and accretion models. For instance, the existence of IMBHs is a channel for the formation of 10^{4-5} $M_\odot$ BHs, which are thought to be relevant for the presence of supermassive BHs in quasars at $z > 6$–7 (Pacucci, Natarajan, & Ferrara , 2017).

While these discoveries represented an important step forward in the understanding of pulsars at high accretion rate regimes, their timing properties also opened new issues related to the detection algorithms used to search for coherent signals. In fact, the high accretion rates of PULXs have a strong impact on the absolute value of the torque acting onto the NS due to the interaction between the accretion stream and the magnetosphere, resulting in a very high spin-up rate (with $|\dot{P}|$ in the range 10^{-7}–10^{-10} s s^{-1}). Additionally, the greatest part of PULXs have orbital periods of 2-5days, a value comparable with the typical observational baseline (∼2days for mission like XMM-Newton and Chandra). Both effects play an important role in eventually washing out a signal too much to be corrected with standard search algorithms.

The ULTraS and PulsULTraS projects allowed us to focus on a number of important issues related to the above topics. In particular, we:

- developed new timing analysis tools aimed at largely improving our capability of detecting fast (<10s-period) and rapidly changing coherent signals (Sec. 3). We also started to import our new *ad hoc* software within the open-source software package `Stingray` (Sec. 8);
- addressed the problem related to the occurrence percentage of PULXs among ULXs by submitting a Large Program to XMM-

Newton (accepted in 2018) in order to at least double the number of ULXs over which it is possible to search for pulsations with parameters similar to those already observed from PULXs (Sec. 4);
- extended our understanding of the PULX phenomenon by submitting several (Large) Programs to XMM-Newton and NuSTAR (carried out between 2018-2021) in order to study in great details the other known PULXs: M 82 X-2, NGC 7793 P13 and NGC 5907 ULX-1 (Sec. 5 and 6);
- performed a systematic search for X-ray signals by applying a sort of acceleration algorithm over about 72000 light curves extracted from the XMM-Newton archive (Sec. 7).

3. Software development

Based on the timing properties of known PULXs we decided to set a number of *ad hoc* pipelines aimed at taking into account the possible presence of a strong first period derivative of the putative signal and/or an orbital motion of the compact object (causing the signal) around its companion star. The first step was to account for an unknown $\dot{P}$ value affecting an unknown signal. The expected correction, in term of event arrival times, is given by t'=t-1/2($\dot{P}/P$)t^2, where t is the observed time. It is therefore possible to apply different corrections for each time series (light curve) for different values of the parameter $\dot{P}/P$. For each correction a Power Spectrum Density (PSD) is carried out and searched for significant peaks. A similar approach can be also considered to correct for the effects due to an unknown (circular) orbit, where t'=t-$a_x sin\, i[2\pi(t - T_{asc})/P_{orb}]$, where $a_x sin\, i$, P_{orb} and T_{asc} are the projection of the semi-axis, the orbital period and the time of the ascending node, respectively (the more general case of an elliptical orbits can be also taken into account by including two additional free parameters, the ellipticity e and the time of the periastron passage). Finally, for each orbital correction a further $\dot{P}/P$ correction can be also considered. It is evident that this approach implies up to millions corrections (in the most extreme cases) for each time series and it might be high CPU-consuming.

3.1. M31 and the post-EXTraS search

The above described algorithms/pipelines were first applied to the XMM-Newton archival observations of the nearby galaxy M31 both to test their capability of recovering the already known pulsators detected within the *EXTraS* project (3XMM J004301.4+413017, 1.2 s period, and 3XMM J004222.9+411535, 464 s period; see De Luca et al. 2021 and upper insets of Figure 1) and to search for new pulsators missed by EXTraS due to their orbital motion and/or strong $\dot{P}$. The analysis was performed by means of the High Performing Computers (HPCs) provided by CINECA and INAF (through the CHIPP pilot project). During the search a previously unknown coherent signal at about 3 s popped-up in 9 out of 49 XMM-Newton datasets (see lower inset of Figure 1) of the source 3XMM J004232.1+411314, a bright hard X-ray source located at 3.7' from the bulge of M31, and known to show dips with an orbital period of about 4.01 hr (Rodríguez Castillo et al. , 2018; Marelli et al. , 2017). 3XMM J004222.9+411535 is another milestone in the study of extragalactic X-ray pulsars. It is the first low-mass X-ray binary likely hosting a young magnetised neutron star outside the Milky Way, a rare evolutionary path for a binary system. Alternatively, it might be a mildly magnetised NS rotating close to P_{eq}.

Furthermore, we extended the search for coherent signals carried out during the *EXTraS* project also to about 4800 new archival XMM-Newton datasets (about 1.3 millions PSDs analysed): it resulted in the discovery of further 12 new X-ray pulsators. The whole sample of new pulsators discovered by *EXTraS* and post-*EXTraS* have similarities but also interesting differences with respect to that identified in the Chandra archive which will be presented and discussed in a dedicated paper (Israel et al. 2016 and Rodríguez Castillo et al., in preparation).

3.2. A Python implementation for the `accelsearch` algorithm

Ransom et al. (2002) presented a fast Fourier-based algorithm for the search of accelerated pulsations in radio data. This algorithm is implemented in `PRESTO`[2] and has been extensively used for accelerated radio pulsar searches. Whereas most algorithms for acceleration correction correct the times in the time series, and run the periodicity detection algorithm on the corrected data (based on the FFT or another statistic), the Fourier-domain accelerated search (known as `accelsearch`) acts directly on the Fourier representation of the data. A sinusoidal signal with a constant frequency has a Fourier response described by a sinc function (Van Der Klis , 1989). In the presence of acceleration, i.e. a constant change of frequency, this response will be spread over multiple bins of the Fourier transform. It can be shown that the spread is described by the convolution between the sinc response and a finite impulse response (FIR) filter. The accelsearch method calculates only one FFT of the uncorrected data, and corrects for the spread of the signal in multiple FFT bins through the correlation with a frequency-reversed and complex-conjugated template that reverses the effect of the acceleration. These correlations can be computed very quickly, thanks to a large literature of methods to speed up and parallelize the convolutions. This algorithm has been used for a long time in radio pulsar searches where running accelerated searches on larger-than-RAM dataset was crucial. We implemented the algorithm in pure Python (Pisanu , 2020) and added it to the `Stingray` library in 2020, sped it up through a number of techniques including, but not limited to, *just-in-time compilation*[3], and used it since then for accelerated searches in multiple observations of candidate PULXs. Future plans include the addition of second order acceleration search (or "jerk" search), as described by Andersen & Ransom (2018)

[2] https://github.com/scottransom/presto

[3] Through the `numba` library, `https://numba.pydata.org/`

4. The UNSEEN program and the PULX in M51

It is evident, from what above outlined, that a major step forward in the study and understanding of ULXs goes through the expansion of the sample of ULXs where a sensitive search for pulsations can be carried out. With this aim, in 2018 we carried out a series of XMM-Newton observations aimed at doubling up the sample of ULXs with a good statistics where to search for signals and therefore assessing the incidence of ULX Neutron Star Extreme Extragalactic populatioN (UNSEEN) among ULXs. Figure 3 summarizes the systematic and automatic signal search procedure we adopted within the UNSEEN project making use of the pipelines outlined in section 3. For each targeted ULX, coherent signals are first searched in raw data (with no corrections for the $\dot{P}$ or the orbital motion; red squared plot labelled "Raw data") by means of a PSD where Fourier resolution and Nyquist frequency are maximized and the possible presence of non-Poissonian noise components is taken into account (see Israel & Stella 1996 for more details). If no signal is found during this first step, a grid of 1-dimension $\dot{P}/P$ values is applied to the source event times; for each $\dot{P}/P$ value a PSD is obtained and a corresponding plane P versus $\dot{P}$ is obtained as a function of the power estimates (see blue squared plots in Fig. 3 labelled "1D correction"; the shown PSD corresponds to the $\dot{P}/P$ value providing the highest power estimate). In the case reported in Figure 3 a significant peak is found above the 3.5σ detection threshold (blue solid line). Once a candidate signal is identified a refined timing analysis is carried out by assuming a 3-dimension grid of (circular) orbital parameters, i.e. the orbital period P_{orb}, the semi major axis projection $a_x \sin i$, and the time of the ascendant node T_{node}. Each set of orbital parameters is used to modify the arrival times of source events and a PSD is carried out. In the case reported in Figure 3 we plot two parameters as a function of the PSD power estimate: P_{orb} versus $a_x \sin i$ (green squared plots labelled "3D correction").

The example reported in Figure 3 refers to the discovery, within the UNSEEN project, of

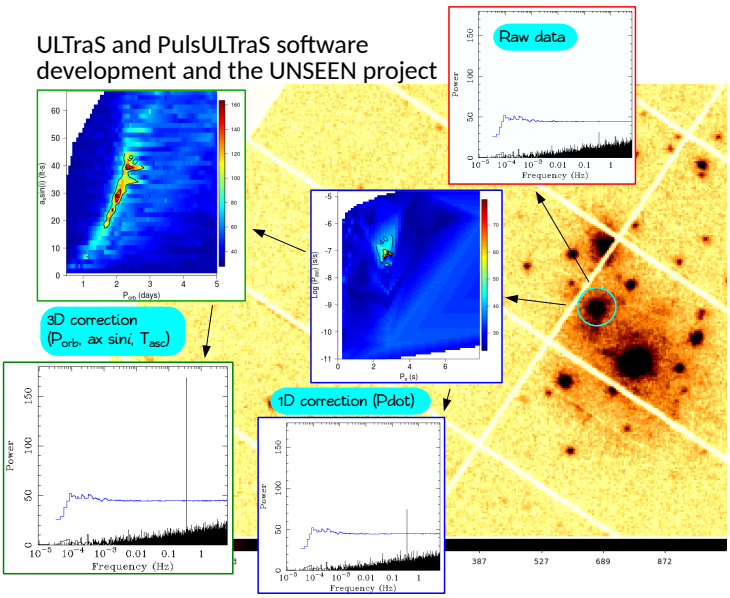

Fig. 3. Signal discovery procedure adopted for the UNSEEN project referring to the XMM-Newton pn data of M51 (ObsId 0824450901). For each targeted ULX, a "raw" PSD is carried out (red squared inset), then a plot is obtained where each point in the plane P-$\dot{P}$ corresponds to the power of the highest peak found in PSDs obtained by correcting the photon arrival times with values in the -11< |Log($\dot{P}$/P)| <-5 range (blue squared insets). Colors mark the Leahy power estimates in the corresponding PSD (intensity scale on the right). For the $\dot{P}$ value corresponding to the highest power estimate, a PSD is also shown. In the final step of the procedure the source photon arrival times are corrected for the Doppler effect originated by an orbital motion. We show the orbital period as a function of $a_x \sin i$ together with the best orbital parameter PSD (green squared insets). Adapted from Israel & Rodriguez Castillo (2019).

the new PULX in the M51 galaxy, namely M51 ULX7, first detected with ROSAT observations at a luminosity above 10^{39} erg s^{-1}. In fact pulsations at a period of 2.8 s were discovered in three XMM-Newton observations carried out in May-June 2018 . The pulse shape is sinusoidal and large variations of its amplitude were observed even within single exposures (pulsed fraction from less than 5% up to 20%). The signal disappeared (3σ upper limits on the pulsed fraction of about 3%) for at least 3hr at the end of one of the XMM pointings. Furthermore, the X-ray pulsar revolves in a 2-days orbital period binary with a projected semi-major axis $a_x \sin i \simeq 28$ lt-s Rodríguez Castillo et al. (2020). For a neutron star of 1.4 $M_\odot$, this implies a lower limit on the companion mass of 8 $M_\odot$, suggesting that the system consists of an OB giant and a moderately magnetic (dipole field component in the range 10^{12} G $\leq B_{dip} \leq 10^{13}$ G) accreting NS with weakly beamed emission ($1/12 \leq b \leq 1/4$).

5. NGC5907 ULX-1

This PULXs plays a crucial role in the understanding of the class being by far the one with the largest super-Eddington luminosity (and therefore the highest accretion rate). In the past years we activated a number of observational programs aimed at better constraining the orbital parameters and at checking the onset of a magnetic gate scenario to account for the observed high-low flux switches. During one of these campagins the source dimmed by more than a factor of 50 in flux. A subsequent deep Chandra pointing revealed an ex-

tended source at the position of the pulsar. The extended structure has been interpreted as an expanding nebula powered by the wind of the pulsar (diameter of about 200 pc and L_X of about 2×10^{38}erg s^{-1}) implying a power of 1.3×10^{41}erg s^{-1} and a characteristic age of about 7×10^4 yr. This interpretation suggests that a genuinely super-Eddington regime can be sustained for time scales much longer than the spin-up time of the neutron star powering the system and making the PULX phase longer than thought before (Belfiore et al. , 2020). Further pointings obtained in 2019-2021 when the source resumed form the low flux state showed that the period has spun-down, confirming that the pulsar experienced a genuine halt of the accretion and entered into a propeller phase (Fürst et al., in preparation).

6. More ULX timing with XMM-Newton and NuSTAR

Besides the main objective of this project, we gave multiple levels of support for the scientific interpretation and the timing analysis of other PULXs, for example leading the analysis of XMM-Newton data in multi-instrument projects, and/or verifying timing results obtained with other software packages. An example of the latter is a large NuSTAR campaign on M82 X-2, that led to the determination of a very precise ephemeris (Bachetti et al. , 2021) and later to the first detection of an orbital period decay in a PULX (Bachetti et al. , 2021). Further broadband studies on the periodic and aperiodic timing properties and M82 X-2 are being enabled by quasi-simultaneous XMM-Newton and NuSTAR observations conducted in 2020 and 2021, that will be described in a paper currently in preparation. Similarly, we provided an independent verification for the peculiar timing results on NGC 7793 P13 obtained with a long campaign involving Swift/XRT, Swift/UVOT, XMM-Newton, and NuSTAR (Fürst et al. , 2021). The pulsar shows two very similar, but distinct, ~65-day modulations in the pulsar period and UV and X-ray light curves. Whereas the pulse period is easy to attribute to the orbit, the origin of the modulations at X and UV energies with slightly different periods is unclear. Also, P13 showed, similarly to NGC 300 ULX1 (e.g. Vasilopoulos et al. 2019), a drop of flux during which the spin-up remained stable. This implies that the flux was not due to a decrease of accretion rate, but probably to some material (partially) hiding the source.

7. Searches with acceleration algorithms

Encouraged by the results obtained within the *EXTraS* project and the systematic application of our *ad hoc* timing analysis pipelines, we decided to make one more step forward and to systematically search for new periodic signals, with the help of acceleration algorithms, in a sub-sample of the EXTraS archival time series. To maximise the probability of finding new pulsators and to minimize the CPU-time, we applied the following requests:

- sources on the galactic plane ($|b| < 20^\circ$) or in one of the Magellanic Clouds or in M31;
- time series consisting of at least 500 photons, so that the minimum pulsed fraction detectable at a 3.5σ level can be $< 40\%$.

We found ~72,000 time series complying to the above requests. For each time series in the sample we tested ~2,000 trial values of the parameter $\dot{P}/P$ in the range $10^{-11}\ s^{-1} < |\dot{P}/P| < 5\times10^{-5}\ s^{-1}$ and for each correction the corresponding PSD has been searched for peaks exceeding the 3.5σ probability threshold for periods shorter than $1000\ s$. As far as we know, this was the first time that a similar approach was considered for such a large sample in the X-rays (Imbrogno et al., in preparation).

A way to disentangle genuine signals from noise fluctuations relies upon the signal properties. In fact as the correction approaches the best one for the given time series the corresponding power in the PSD increases, reaches a maximum value and then decreases (at variance with a statistical fluctuation peak which does not depend on the $\dot{P}/P$ correction). This effect can be seen in Figure 4 where every point corresponds to the peak with the highest power found by the pipeline in a single correction of one of the analysed time series.

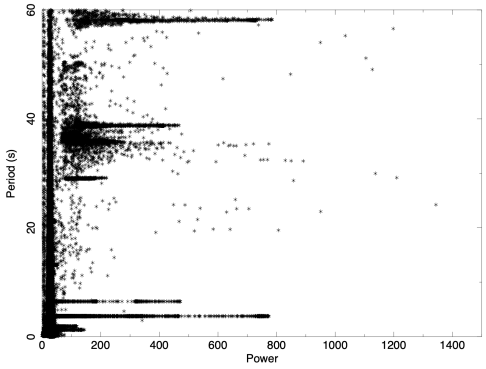

Fig. 4. Best period P found by the acceleration algorithm for every $\dot{P}/P$ correction of a sub-sample of the selected time series versus the power of the highest peak. The "rows" indicate genuine signals for which subsequent corrections increase the power at a given period, until an optimum correction is reached and the power starts to decrease.

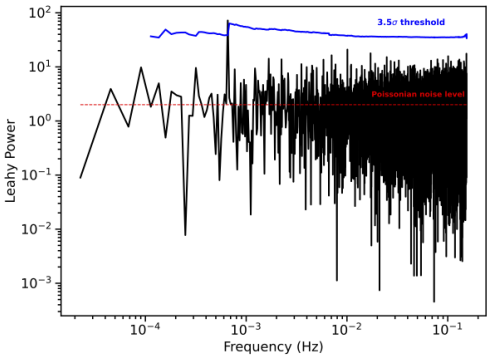

Fig. 5. CHANDRA/ACIS Fourier power spectrum of CXOU J112347.4–591834 (Israel et al., 2016) (Obs. id 126) obtained with our *ad hoc* algorithms imported within `Stingray`. The blue line corresponds to the 3.5σ confidence level threshold for potential signals, computed taking into account the number of frequency bins of the spectrum. The peak above the threshold corresponds to the ∼1522 s period. The red dashed line corresponds to the Poissionian noise level.

We found 95 time series from unknown sources with a significant peak exceeding the 3.5σ detection threshold in at least two contiguous $\dot{P}/P$ corrections, and tagged them as candidate signals for further studies. This analysis is still on going.

8. Further software development

In order to make accessible to the scientific community the search algorithms we developed and used in the EXTraS/UNSEEN projects, we decided to include them in the `Stingray` software package[4] (Huppenkothen et al., 2019). Some of the routines of the code are being rewritten and updated and we are implementing a Python wrapper that will allow to call the original Fortran subroutines of the Israel & Stella (1996) code into `Stingray`. Once the merging of the two codes is completed we will make the software publicly available. It will be released as part of the HENDRICS command-line scripts[5] based on `Stingray`. The code will include different algorithms for the computation of power spectra and the search of different types of variability on each time series. The search for coherent pulsations will be performed by looking for peaks in the power spectrum that exceed a given detection threshold. In the absence of significant peaks, an upper limit on the amplitude of a sinusoidal modulation will be calculated for each frequency. The first version of the code is being tested for X-ray data, but the final version will also work for optical and UV time series starting from FITS event files. An example of the code output is shown in Fig.5. The search algorithm identifies one peak above the 3.5σ detection threshold (solid blue line) that corresponds to the CXOU J112347.4–591834 source (Israel et al., 2016) with a periodicity of ∼1522 s. The Leahy normalized power of 72.1 corresponds to a detection at $6.0\,\sigma$ level. The threshold for potential signals is computed taking into account the number of frequency bins of the spectrum and the possible presence of additional non-Poissonian noise components in the PSD.

[4] `https://github.com/StingraySoftware/stingray`

[5] `https://https://hendrics.stingray.science/en/latest/`

9. Conclusions

The discovery of the rapidly growing class of PULXs in the latest years has changed our understanding of the ULX class. The detailed study of known PULXs allowed us to realize that their timing properties are even more extreme than thought before, since the detection of their signals is not only hampered by the Doppler effect and by a strong $\dot{P}$; in fact the rapidly changing pulsed fraction of the signals which varies form 20% down to lower than few per cent within few hours is a further obstacle to the discovery of new PULXs. On the other hand all these findings suggest that the number of PULXs among ULXs is even larger than before, likely above 50% of the whole population. In this respect the development and systematic application of *ad hoc* timing tools might be the game-changer in sizing the PULX population, and more in general in detecting extreme timing properties pulsars also in the Milky Way.

Acknowledgements. We acknowledge financial support from ASI under ASI/INAF agreement N.2017-14.H.0 (ULTraS and PULSULTraS projects). This research has made use of data produced by the EXTraS project, funded by the European Union's Seventh Framework Programme under grant agreement no 607452. This project has made use of high performing computing resources under the coordination of the CHIPP project and through resources awarded by CINECA.

References

Andersen, B. C. & Ransom, S. M., 2018, ApJ, 863, L13

Bachetti M., Harrison F. A., Walton D. J., Grefenstette B. W., Chakrabarty D., Fürst F., Barret D., et al., 2014, Nature, 514, 202.

Bachetti M., Maccarone T. J., Brightman M., et al. 2020, ApJ, 891, 44

Bachetti M., Heida M., Maccarone T., et al. 2021 arXiv:2112:00339

Belfiore A., Esposito P., Pintore F., Novara G., Salvaterra R., De Luca A., Tiengo A., et al., 2020, Nature Astronomy, 4, 147. doi:10.1038/s41550-019-0903-z

Chashkina A., Abolmasov P., Poutanen J., 2017, MNRAS, 470, 2799.

De Luca, A. et al. 2021, A&A, 650, A167.

Esposito P., Israel G. L., Belfiore A., Novara G., Sidoli L., Rodríguez Castillo G. A., De Luca A., et al., 2016, MNRAS, 457, L5.

Fürst F., Walton D. J., Harrison F. A., Stern D., Barret D., Brightman M., Fabian A. C., et al., 2016, ApJL, 831, L14.

Fürst F., Walton D. J. Heida, M., et al. 2021, arXiv:2105:04229

Huppenkothen, D., Bachetti, M., Stevens, A. L., et al. 2019, ApJ, 881, 39.

Israel, G. L. & Stella, L. 1996, ApJ, 468, 369.

Israel, G. L., Esposito, P., Rodríguez Castillo, G. A., et al. 2016, MNRAS, 462, 4371.

Israel G. L., Belfiore A., Stella L., Esposito P., Casella P., De Luca A., Marelli M., et al., 2017, Sci, 355, 817.

Israel G. L., Papitto A., Esposito P., Stella L., Zampieri L., Belfiore A., Rodríguez Castillo G. A., et al., 2017, MNRAS, 466, L48.

Israel G. L., Rodriguez Castillo G. A., UNSEEN Collaboration, 2019, MmSAI, 90, 216

Leahy, D. A. et al. 1983, ApJ, 266, 160L.

Marelli M., Tiengo A., De Luca A., Salvetti D., Saronni L., Sidoli L., Paizis A., et al., 2017, ApJL, 851, L27.

Pacucci F., Natarajan P., Ferrara A., 2017, ApJL, 835, L36.

Pisanu F., 2020, Master's Degree Thesis, Universitá degli Studi di Cagliari, Italy.

Ransom S. M., Eikenberry S. S. and Middleditch J., 2002, ApJ, 124, 1788

Rodríguez Castillo, G. A. et al. 2020, ApJ, 895, 60.

Rodríguez Castillo G. A., Israel G. L., Esposito P., Papitto A., Stella L., Tiengo A., De Luca A., et al., 2018, ApJL, 861, L26.

Trudolyubov S. P., Priedhorsky W. C., Córdova F. A., 2007, ApJ, 663, 487.

Trudolyubov S. P., 2008, MNRAS, 387, L36.

Trudolyubov S. P., 2013, MNRAS, 435, 3326.

Van Der Klis M., 1989, in "Timing Neutron Stars"

Vasilopoulos G., Petropoulou M., Koliopanos F., et al. 2019, MNRAS, 488, 5225

Zolotukhin I. Y., Bachetti M., Sartore N., Chilingarian I. V., Webb N. A., 2017, ApJ, 839, 125.